Surface plasmon resonance and circular dichroism characterization of cucurbitacins binding to serum albumins for early pharmacokinetic profiling

Edoardo Fabini[1], Giovana Maria Lanchoti Fiori[2], Daniele Tedesco[1], Norberto Peporine Lopes[2], Carlo Bertucci[1*]

[1] *Department of Pharmacy and Biotechnology, University of Bologna, Via Belmeloro 6, 40126 Bologna, Italy.*

[2] *Department of Physics and Chemistry, Faculty of Pharmaceutical Sciences of Ribeirão Preto, University of São Paulo, Ribeirão Preto, CEP 14049-900, Brazil.*

[*] *Corresponding author. Telephone: +39 0512099731. Fax: +39 0512099734. Email: carlo.bertucci@unibo.it*

Accepted Manuscript version. The Published Journal Article is available on the Journal of Pharmaceutical and Biomedical Analysis, *Volume 122, pages 166–172 (DOI: https://doi.org/10.1016/j.jpba.2016.01.051). Supplementary Material available free of charge on the article webpage.*

Abstract

Cucurbitacins are a group of tetracyclic triterpenoids, known for centuries for their anti-cancer and anti-inflammatory properties, which are being actively investigated over the past decades in order to elucidate their mechanism of action. In perspective of being used as therapeutic molecules, a pharmacokinetic characterization is crucial to assess the affinity towards blood carrier proteins and extrapolate distribution volumes. Usually, pharmacokinetic data are first collected on animal models and later translated to humans; therefore, an early characterization of the interaction with carrier proteins from different species is highly desirable. In the present study, the interactions of cucurbitacins E and I with human and rat serum albumins (HSA and RSA) were investigated by means of surface plasmon resonance (SPR)-based optical biosensing and circular dichroism (CD) spectroscopy. Active HSA and RSA sensor chip surfaces were prepared through an amine coupling reaction protocol, and the equilibrium dissociation constants (K_d) for the different cucurbitacins-serum albumins complexes were then determined by SPR analysis. Further information on the binding of cucurbitacins to serum albumins was obtained by CD competition experiments with biliverdin, a specific marker binding to subdomain IB of HSA. SPR data unveiled a previously unreported binding event between CucI and HSA; the determined binding affinities of both compounds were slightly higher for RSA with respect to HSA, even though all the compounds can be ranked as high-affinity binders for both carriers. CD analysis showed that the two cucurbitacins modify the binding of biliverdin to serum albumins through opposite allosteric modulation (positive for HSA, negative for RSA), confirming the need for caution in the translation of pharmacokinetic data across species.

Keywords

SPR optical biosensor; Circular dichroism; Drug binding; Cucurbitacins; Serum albumins; Binding affinity.

1. Introduction

Cucurbitacins (Cuc) are a class of highly oxygenated, tetracyclic triterpenoids primarily isolated from the plant family of Cucurbitacee. The cytotoxicity of cucurbitacins has been known for centuries and the elucidation of their mechanism of action is an active topic of research; several biological and pharmacological activities have been reported, proposing cucurbitacins as potential anti-cancer, anti-inflammatory and anti-microbial agents [1-4]. For instance, cucurbitacin E (CucE, Fig. 1) disrupts the F-actin cytoskeleton, inhibiting the growth of human prostate carcinoma PC-3 cells [5], and displays anti-angiogenesis activity in human umbilical vascular endothelial cells by suppressing the VEGFR2-mediated Jak2–STAT3 signaling pathway [6]; cucurbitacin I (CucI, Fig. 1), the deacetylated form of CucE, induces apoptosis in Sézary syndrome cells through the inhibition of the same pathway [7] and displays cardioprotective properties through the suppression of the tissue growth factor-mediated signaling pathways in hypertrophic cardiomyocytes [8]. In view of the potential use of cucurbitacins as therapeutic agents, binding studies with carrier proteins, and in particular with serum albumins, are highly desirable in order to better characterize their distribution and bioavailability for their primary targets, and therefore understand their pharmacological behavior.

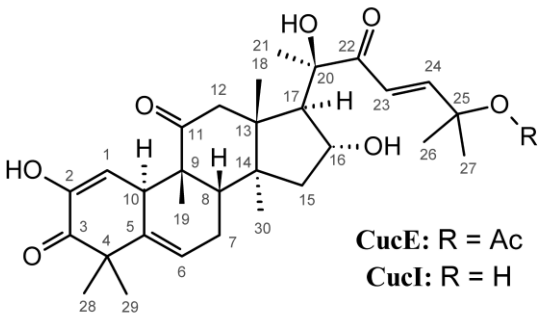

Figure 1. Chemical structures of CucE and CucI.

Human serum albumin (HSA) is the most abundant protein carrier in blood serum [9]. HSA possesses the ability to bind to several different classes of compounds, either endogenous and exogenous, modulating their properties such as solubility, availability, toxicity and stability [9].

Several techniques have been successfully applied to characterize the binding properties of HSA, e.g. equilibrium dialysis, high-performance affinity chromatography and fluorescence spectroscopy to name a few [10-15]. Among these, circular dichroism (CD) spectroscopy [16, 17] offers the analytical advantages given by its trademark sensitivity to chirality, allowing the investigation of binding events through the phenomenon of induced circular dichroism (ICD). The occurrence of ICD is the result of strong, stereospecific binding phenomena between interacting molecules, whose chiroptical properties are consequently modified through conformational restraint and electronic coupling between the chromophores of both guest and host molecules [18]; the ICD signals of specific high-affinity markers for the binding sites of HSA can therefore be exploited to characterize the binding of other analytes by means of competition studies in solution [19, 20].

Optical biosensors based on surface plasmon resonance (SPR) have also been employed during the last years in order to study the interaction between small molecules and proteins [21-24]. In a typical SPR experiment, one of the two binding partners is chemically attached to the surface of a sensor chip (ligand), while the other is free to flow in solution (analyte) and is thus able to interact with the ligand. The response (*R*), given in arbitrary resonance units (RU), is dependent on the refractive index of the chip surface, which varies proportionally to the change in mass due to the association and/or dissociation of the binding complex between ligand and analyte. This technique offers advantages over the conventional solution-based techniques:

(a) the interaction between two molecules can be monitored without the need of any labeling, obtaining binding information about unmodified reactants and avoiding the possibility to alter the binding properties [25];

(b) sensor chips can be used for several cycles of analysis without compromising their functionality, therefore increasing the throughput of the technique [26];

(c) unlike other equilibrium-based techniques, the interaction can be monitored in real time, providing more detailed information about the binding process [27].

The latter feature is of particular interest when monitoring biological systems, especially when dealing with carrier proteins, since the kinetics of binding greatly influences the pharmacokinetic properties of the bound molecules [28].

During pre-clinical and clinical trials, animal models are routinely used to test the binding properties and the consequent bloodstream distribution of new drug candidates in order to extrapolate pharmacokinetic data for the human body [29]. Though HSA and rat serum albumin (RSA) share a high degree of homology in their amino acid sequences, differences in their binding properties has already been demonstrated [30]. Therefore, the investigation of the binding differences among serum albumins from different species becomes of great importance before extrapolating data for clinical studies in humans. Exploiting the versatility of the experimental setup given by SPR-based biosensors, evaluations on the binding properties of different compounds toward immobilized serum albumins from different species can be achieved and compared with data obtained from other solution-based affinity techniques [21].

In the present study, cucurbitacins–serum albumins (Cuc–SA) binding complexes were investigated by means of a combination of SPR-based optical biosensing and CD spectroscopic analysis, with particular focus on the binding of CucE and CucI with HSA and RSA.

2. Materials and methods

2.1. Materials

Cucurbitacin E (CucE; molecular weight, MW: 556.76 Da) and cucurbitacin I (CucI; MW: 514.16 Da) were purchased from Extrasynthese (Genay, France).

HSA (essentially fatty acid free, ≥ 96%, product code A1887; MW: 66.4 kDa), RSA (essentially fatty acid free, essentially globulin free, ≥ 99%, product code A6414; MW: 64.6 kDa), sodium dihydrogen phosphate (NaH_2PO_4), disodium hydrogen phosphate (Na_2HPO_4), dimethyl sulfoxide (DMSO), sodium naproxen (MW: 252.24 Da), (*S*)-warfarin (MW: 308.33), biliverdin hydrochloride (BV; MW: 619.12), sodium chloride (NaCl) and sodium acetate were all purchased from Sigma–Aldrich (Milan, Italy).

Research-grade CM 5 sensor chips, 10X phosphate buffer saline (PBS) and the amine coupling kit, consisting in *N*-ethyl-*N*-(3-dimethylaminopropyl)-carbodiimide (EDC), *N*-hydroxysuccinimide (NHS) and ethanolamine hydrochloride (pH 8.5; 1 M), were all purchased from GE Healthcare Bio-Sciences (Uppsala, Sweden).

Water was bi-distillated, de-ionized, filtered and degassed by Millipore Elix 10. Phosphate buffer (PB) (20 mM) + NaCl (150 mM) (pH 7.4) (running buffer A) was used for the immobilization procedure, while 1X PBS–DMSO (95:5, v/v) (pH* 7.4) (running buffer B) was used for the Cuc–SA interaction studies. All buffer solutions were freshly prepared prior to the analysis and filtered through a 0.22-μm pore size membrane made of a mixture of cellulose nitrate and acetate.

2.2. SPR analysis

2.2.1. Instrumentation

SPR measurements were performed with a Biacore™ X100 system (GE Healthcare Bio-Sciences, Uppsala, Sweden) equipped with an in-line degasser and thermostated at 25 °C. Data were analyzed and processed using the Biacore™ X100 2.0 evaluation software.

2.2.2. Surface preparation and validation

Stock solutions of HSA at a 30 μg mL^{-1} concentration were prepared in sodium acetate buffers (10 mM) at various pH values (pH 4.0, 4.5, 5.0 and 5.5), and the electrostatic pre-concentration at the chip surface was evaluated by injecting each stock solution for 180 s at a 5 μL min^{-1} flow rate, after which the baseline was re-established by injecting a NaOH solution (50 mM). The best condition was achieved using the pH 5.0 stock solution.

Consequently, HSA was immobilized on two CM 5 sensor chips via amine coupling according to the standard Biacore procedure, using the pH 5.0 stock solution. Briefly, the chips were equilibrated at room temperature for 30 min before docking, then the system was primed three consecutive times with running buffer A. The carboxymethyl dextran matrix was activated on both channels of the sensor chip by injecting a freshly prepared mixture of EDC (0.4 M)–NHS (0.1 M) (1:1, v/v) at a 5 μL min^{-1} flow rate for 7 min. Then, the pH 5.0 stock solution of HSA was injected over the active flow cell until the desired amount of immobilized protein was reached, i.e. 9000 RU for the first sensor chip (hereafter referred to as high-density chip) and 5000 RU for the second (low-density chip), while running buffer A was injected over the reference flow cell in order to create a surface to account for non-specific binding events. Finally, the remaining active esters were quenched by injecting ethanolamine hydrochloride for 7 min at a 5 μL min^{-1} flow rate (Fig. S1 in the Supplementary Material). At the end of the whole procedure, the surfaces were allowed to stabilize overnight and, after several buffer injections, a steady baseline was achieved. A single RSA surface was prepared following the same protocol and resulted in an immobilization level of around 8500 RU.

The affinities of naproxen toward HSA and (*S*)-warfarin toward HSA and RSA were evaluated in order to confirm the correctness of the immobilization procedure and validate the binding capacity of the chip surfaces. 1 mg mL^{-1} stock solutions of (*S*)-warfarin and naproxen in DMSO were diluted 1:20 (v/v) using 1X PBS to a final concentration of 162 µM and 198 µM, respectively, in running buffer B (pH* 7.4). These solutions were further diluted using running buffer B and injected over the surface at a 30 µL min^{-1} flow rate; association was allowed for 60 s and dissociation was monitored for 120 s.

2.2.3. Solvent refractive index correction

Since DMSO has a high refractive index (addition of 1 % DMSO gives a bulk response of around 1200 RU), a solvent correction procedure [21] was performed to account for the small variations of DMSO percentage between samples and in the preparation of running buffers. Eight running buffers, consisting of 1X PBS mixed with different amounts of DMSO ranging from 4.5% to 5.8% (v/v) (pH* 7.4), were injected over the active and reference flow cells and a calibration curve was obtained. This procedure is very important while working with small molecules–macromolecules interactions, especially when the ligand is immobilized at high density (5000 RU or more). In this experimental set-up, the expected response has the same magnitude as, or lower magnitude than, the signal arising from refractive index mismatches, therefore including a correction protocol during the evaluation of the data becomes of great significance.

2.2.4. Sample preparation

2 mg mL^{-1} stock solutions of CucE and CucI were prepared in DMSO and stored at −20 °C. The stock solutions were then diluted 1:20 (v/v) each day immediately before analysis using 1X PBS, resulting into a final concentration of 50 µg mL^{-1} in running buffer B (pH* 7.4) for both cucurbitacins. All further dilutions were made using freshly prepared running buffer B.

2.2.5. Analysis of Cuc–SA interactions

Affinity assays were carried out during the same day for both cucurbitacins at 25 °C. The flow rate was set at 30 µL min^{-1} and kept constant throughout all the analyses. For the high-density HSA chip and for the RSA chip, association and dissociation were monitored for 60 s and 120 s, respectively, after which additional 300 s of running buffer B (pH* 7.4) were flowed. Every three cycles, a blank injection was performed in order to monitor the baseline stability and account for systematic and random variations. A concentration range from 3.0 µM to 0.04 µM, obtained by a series of two-fold dilutions, were used in order to assess the affinity of CucE and CucI for both serum albumins.

Data for the Cuc–HSA interactions were also collected onto the low-density HSA chip surface, using a concentration range from 9.0 µM to 0.05 µM in a series of four-fold dilutions. Association and dissociation were both monitored for 30 s; subsequently, 120 s of running buffer B (pH* 7.4) were flowed over the surface in order to monitor the stability of the baseline.

2.2.6. Data analysis

Sensorgram datasets for CucE, CucI, naproxen and (*S*)-warfarin binding to serum albumins were processed according to the same protocol. The responses from the active flow cell were double-referenced against the responses from the reference flow cell and against an average of all the blank injections taken every three cycles of analysis; finally, the solvent refractive index correction was applied [31]. The resulting responses at equilibrium were fitted to a 1:1 isotherm binding model, defined in Eq. (1), in order to extrapolate the equilibrium dissociation constant (K_d) of the ligand-analyte complex:

$$R_{eq} = R_{max} \cdot c / (K_d + c) + R_{bulk} \quad (1)$$

where K_d is expressed in M, c is the concentration of the analyte (in M), R_{eq} is the SPR response of the binding complex at equilibrium (in RU), R_{max} is the maximum response upon saturation of the

ligand on the sensor chip (in RU), and R_{bulk} is the response due to the bulk contribution of samples (in RU).

Each measurement was replicated at least twice and each dataset was fitted in the binding model independently; the resulting parameters were subsequently averaged and expressed with the corresponding standard deviation. The percentage of binding of cucurbitacins to serum albumins (expressed as the percent fraction of bound drug, x_b) was derived from K_d values following the procedure described by Rich and coworkers [28], assuming a physiological serum albumin concentration of 680 µM and a Cuc concentration of 10 µM, which is the standard concentration used in the majority of dialysis studies reported in literature.

Sensorgrams resulting from the Cuc–HSA interaction were also fitted to a simple 1:1 kinetic interaction model, according to which the K_d value is derived from the ratio between the rate constants for association (k_{on}) and dissociation (k_{off}), as shown in Eq. (2):

$$K_d = k_{off} / k_{on} \quad (2)$$

where k_{on} is expressed in M^{-1} s^{-1} and k_{off} is expressed is s^{-1}. The R_{max}, k_{on} and k_{off} values were considered independent of the injected concentration and therefore globally fitted. The χ^2 parameter was used as a statistical tool to evaluate the closeness of the fitting model to the experimental data. The experimental datasets showing non-negligible residual plots after the statistical fitting were discarded and not taken into account for the determination of the kinetic constants.

2.3 CD analysis

2.3.1. Instrumentation

CD and UV spectroscopic analyses were carried out at 25 °C on a Jasco (Tōkyō, Japan) J-810 spectropolarimeter equipped with a PTC-423S Peltier-type temperature control system, using a 10 mm pathlength quartz cell (Hellma, Milan, Italy), a 2 nm spectral bandwidth, a 0.5 nm data pitch

and an accumulation cycle of 3 runs per measurement. Data were analyzed and processed using the Jasco Spectra Manager 2 software package.

2.3.2. Analysis of Cuc–SA complexes

5 mM stock solutions of CucE and CucI were prepared in DMSO, while stock solutions of HSA (300 μM), RSA (300 μM) and BV (3 mM) were prepared in running buffer B (pH* 7.4).

Samples of cucurbitacins (3.75, 7.5, 15, 30 and 60 μM) were prepared by directly diluting appropriate aliquots of 5 mM stock solutions with running buffer B (pH* 7.4).

Cuc–SA complexes were analyzed at different drug/protein molar ratios (0.25, 0.5, 1, 2 and 4) by diluting the protein stock solution with running buffer B (pH* 7.4) to a concentration of 15 μM and subsequently adding increasing aliquots of Cuc stock solution. The resulting decrease in final protein concentration during all titration experiments never exceeded 1.5%, and the total content of DMSO in the samples never exceeded 6.5% (v/v).

CD and UV spectra of samples were then measured in the 450 – 250 nm spectral range using a 50 nm min^{-1} scanning speed and a 2 s data integration time. The increase in DMSO content did not increase the solvent contribution to the total spectroscopic response of samples in the investigated spectral range; consequently, solvent corrections for the samples of cucurbitacins were performed by subtracting the signal of running buffer B (pH* 7.4). On the other hand, the spectra of drug/protein samples were corrected by subtracting the spectra of serum albumins, in order to evaluate the eventual onset of ICD signals upon binding (Fig. 4).

2.3.3. Competition studies with biliverdin

A similar protocol was used for competition experiments on HSA–biliverdin (BV) complexes (Fig. S4 in the Supplementary Material): HSA and BV were mixed at a molar ratio of 1:1 and diluted to 15 μM in running buffer B (pH* 7.4). Increasing aliquots of Cuc stock solution were subsequently

added to the 1:1 HSA–BV complex in order to obtain different Cuc/SA molar ratios (0.5, 1, 1.5, 2, 3 and 5).

For RSA–BV competition experiments (Fig. S5 in the Supplementary Material), the concentration of the 1:1 protein/marker complex was kept at 7.5 μM in running buffer B (pH* 7.4); subsequently, increasing aliquots of Cuc stock solution were added to the 1:1 RSA–BV complex yielding different Cuc/SA molar ratios (0.33, 0.67, 1, 1.33, 2, 4 and 6).

CD and UV measurements were carried out in the 700 – 250 nm spectral range using a 100 nm min^{-1} scanning speed and a 1 s data integration time; blank corrections were performed by subtracting the spectra of serum albumins from the spectra of protein/marker and drug/protein/marker samples. The effect of CucE and CucI on the ICD signal of BV was monitored at the wavelength of maximum UV absorption for BV, lying at around 385 nm: the relative variations of the corresponding ICD signal (expressed as percentage) with respect to the HSA–BV and RSA–BV complexes were plotted as a function of the Cuc/SA molar ratio (Fig. 5, Tables S3–S4 in the Supplementary Material).

3. Results and discussion

3.1. SPR analysis of Cuc–SA interactions

3.1.1. Surface preparation and validation

The immobilization strategy chosen for the surface preparation was to covalently bind the serum albumins to the carboxymethyl dextran layer of the sensor chips through its primary amine groups using an amine coupling reaction. This strategy is the most used for the study of small molecules–serum albumins interactions as it is known that, in these conditions, HSA exposes its primary binding sites [28]. Prior to the immobilization, a pH scouting procedure was performed in order to determine which solution, at pH values below the isoelectric point (pI) of the protein and above the pI of the carboxymethyl dextran layer of the sensor chip, gave the most stable interactions between the ligand and the chip surface. At pH 5.0, HSA produces a stable and time-dependent interaction, which was optimal to control the immobilization density by setting the adequate injection time at the beginning of the procedure. To confirm the full functionality of produced chip surfaces, naproxen (marker for the Sudlow site II of HSA [10, 11]) and (*S*)-warfarin (Sudlow site I marker) were used as standard compounds to assess their affinity toward the HSA surfaces. In all cases, a good concentration–response relationship was observed and the resulting K_d values (3.6×10^{-5} M for naproxen and 6.0×10^{-6} M for (*S*)-warfarin on the high-density chip surface; 2.5×10^{-5} M µM for naproxen and 3.6×10^{-6} M for (*S*)-warfarin on the low-density chip surface) were in accordance with previously reported SPR analyses (K_d values in the range 3.0×10^{-6} to 2.6×10^{-5} M for naproxen, 3.7×10^{-6} to 1.4×10^{-5} M for (*S*)-warfarin) [21, 28]. The affinity of (*S*)-warfarin toward the RSA surface was also assessed, yielding a K_d value of 2.3×10^{-5} M which is in good agreement with literature data [32].

3.1.2. Affinity of Cuc–SA complexes

All interacting compounds reached the steady state of the reaction within few seconds from the injection and dissociated rapidly from both serum albumins as indicated from the square wave shape of the sensorgrams (Fig. 2).

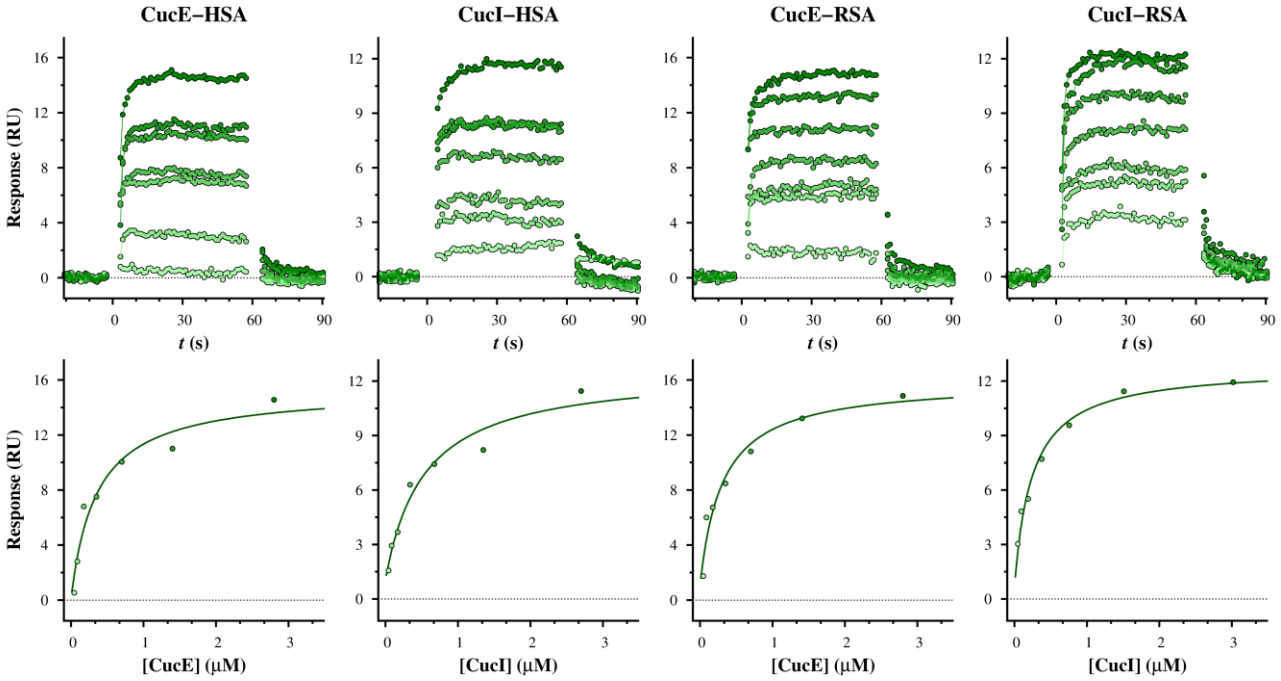

Figure 2. Representative SPR sensorgrams (*top*) and R_{eq} values fitted to the 1:1 isotherm binding model (*bottom*) for CucE and CucI binding to the high-density HSA and RSA chip surfaces. Increasing concentrations of analyte are denoted by different shades of green (*from light to dark*): 0.05, 0.09, 0.18, 0.35, 0.70, 1.40 and 2.80 μM for CucE–HSA; 0.04, 0.08, 0.17, 0.34, 0.68, 1.35 and 2.70 μM for CucI–HSA; 0.05, 0.09, 0.18, 0.35, 0.70, 1.40 and 2.80 μM for CucE–RSA; 0.04, 0.08, 0.17, 0.34, 0.68, 1.35 and 2.70 μM for CucI–RSA.

By decreasing the immobilization level, the R_{max} signals decrease, and the signal-to-noise ratio decreases accordingly; however, the influence of non-specific interactions, such as steric hindrance, crowding and aggregation at the functionalized surface, is also reduced allowing to provide cleaner and more reliable sensorgrams [31]. Furthermore, reproducing biosensor data on different surface preparations gives more reliability to the whole analysis by avoiding surface-dependent artifacts . The low-density HSA chip showed R_{max} values below 10 RU, though all the sensorgrams were spatially discerned and data collected were suitable for a fitting procedure (Fig. S2 in the Supplementary Material). Therefore, the binding affinity of the CucE–HSA interaction, determined by independent experiments on both sensor chips, resulted in an average K_d value of 5.0×10^{-7} M,

which is in good agreement with the literature value of 5.8×10^{-7} M obtained by solution-based fluorimetry assays [33].

The K_d value for the binding of CucI toward HSA was estimated to be 1.8×10^{-6} M, suggesting a previously unreported interaction between the two molecules. On the other hand, both CucE and CucI showed higher affinity toward RSA with respect to HSA, with estimated K_d values of 2.9×10^{-7} M and 2.8×10^{-7} M, respectively. The corresponding x_b values indicate that both cucurbitacins can be ranked as high-affinity binders for HSA and RSA [28]. Results for all the analyzed interactions are reported in Table 1; full details are reported in the Supplementary Material (Table S1).

Table 1. Equilibrium dissociation constants (K_d), kinetic rate constants (k_{on} and k_{off}) and percentages of binding (x_b) derived from the SPR analysis on Cuc–SA binding complexes.

	K_d (M)	k_{on} (M^{-1} s^{-1})	k_{off} (s^{-1})	k_{off} / k_{on} (M)	x_b (%)
CucE–HSA	$(5.0 \pm 1.0) \times 10^{-7}$	$(3.6 \pm 0.7) \times 10^{5}$	$(3.4 \pm 0.7) \times 10^{-1}$ [a]	$(9.5 \pm 1.1) \times 10^{-7}$	99.3 ± 0.1
CucE–RSA	$(2.9 \pm 1.0) \times 10^{-7}$	– [b]	– [b]	– [b]	99.6 ± 0.1
CucI–HSA	$(1.8 \pm 0.7) \times 10^{-6}$	$(4.6 \pm 2.4) \times 10^{4}$	$(1.5 \pm 1.2) \times 10^{-1}$ [a]	$(3.4 \pm 1.5) \times 10^{-6}$	97.4 ± 1.0
CucI–RSA	$(2.8 \pm 0.1) \times 10^{-7}$	– [b]	– [b]	– [b]	99.6 ± 0.1

[a] Numerical value outside the optimal range of work for the instrument. [b] No extrapolation was possible.

The kinetics of binding between cucurbitacins and HSA was then evaluated by applying a 1:1 kinetic interaction model to the SPR datasets, in order to extrapolate the k_{on} and k_{off} rate constants (Fig. 3 and S3 in the Supplementary Material). The residual plots and the χ^2 values were examined to assess the reliability of the theoretical model applied to the experimental data; full details are reported in the Supplementary Material (Table S2). The K_d values derived from Eq. (2) for the Cuc–HSA interactions (9.5×10^{-7} M for CucE, 3.4×10^{-6} M for CucI) were similar to the ones obtained from the steady-state affinity study; on the other hand, the model failed to provide reliable values for the kinetic parameters of Cuc–RSA interactions. The determined kinetic rate constants allow to hypothesize that part of the higher affinity toward HSA displayed by CucE with respect to CucI is due to a 8-fold faster association ($k_{on} = 3.6 \times 10^5$ M^{-1} s^{-1} for CucE, $k_{on} = 5.0 \times 10^4$ M^{-1} s^{-1} for CucI),

although the Biacore evaluation software provided numerical estimates for the k_{off} rate constants which are often outside the optimal range of work of the instrument (Table S1 in the Supplementary Material). As a consequence, the fast nature of this specific dissociation event may require further examination and more advanced techniques to be measured with greater precision.

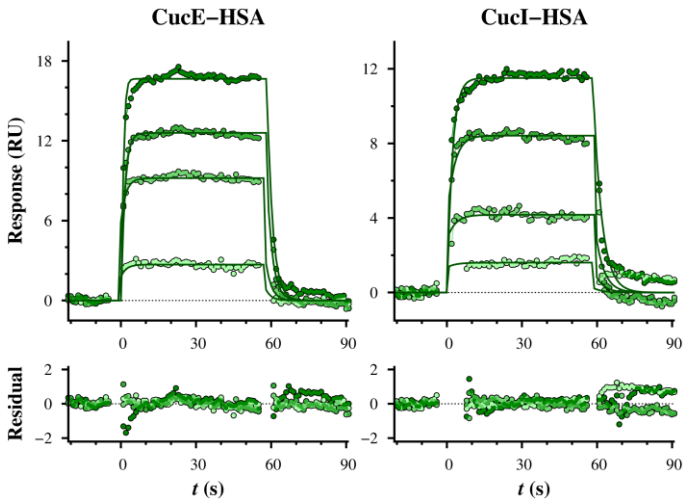

Figure 3. Kinetic fitting of SPR sensorgrams for CucE and CucI binding to the high-density HSA chip surface. Increasing concentrations of analyte are denoted by different shades of green (*from light to dark*): 0.04, 0.18, 0.70 and 2.80 µM for CucE; 0.04, 0.17, 0.68 and 2.70 µM for CucI.

3.2. CD analysis of Cuc–SA interactions

The cucurbitane skeleton of CucE and CucI (Fig. 1) is characterized by the presence of 8 stereogenic centers of defined absolute configuration at positions 8 (*S*), 9 (*R*), 10 (*R*), 13 (*R*), 14 (*S*), 16 (*R*), 17 (*R*) and 20 (*R*). CucE only differs from CucI for the presence of the acetoxy group in place of the hydroxy group at position 25, which is however too distant from the stereogenic centers to be affected by the overall stereochemistry and to display a strong contribution to the chiroptical properties of CucE. The observation of very similar CD signals for CucE and CucI is therefore not surprising (Fig. 4): the spectra in the 450 – 250 nm spectral range are dominated by the $n \rightarrow \pi^*$ of the three ketone chromophores and by the $\pi \rightarrow \pi^*$ transitions of the two α,β-unsaturated ketones, which give rise respectively to a negative CD band centered at 327 nm and a positive CD band centered at 282 nm.

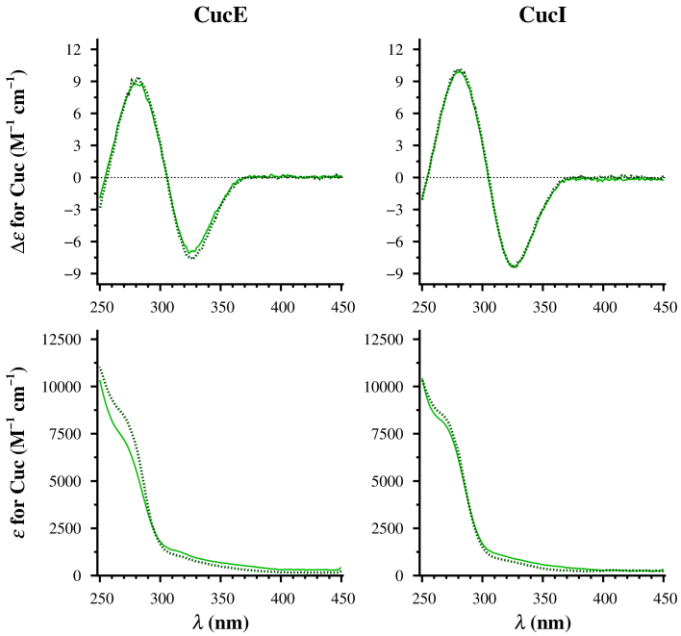

Figure 4. CD and UV spectra of CucE and CucI in solution (*solid lines*) and protein-corrected spectra of their 2:1 complexes with HSA (*dotted lines*). Experimental conditions are reported in the Materials and Methods section.

The $n \rightarrow \pi^*$ CD band of CucE and CucI lies in a spectral region where the spectroscopic contribution of serum albumins is absent, which is an ideal situation for monitoring eventual ICD phenomena. Upon binding to serum albumins, however, the CD profiles of CucE and CucI are not altered, meaning that the binding mechanism is not endowed with a particular stereospecific character (Fig. 4). The position of the CD bands of CucE and CucI is also a huge limitation for the application of CD spectroscopy to the study of Cuc–SA complexes: the usual ICD markers for high-affinity HSA binding (phenylbutazone for the Sudlow site I in subdomain IIA, diazepam for the Sudlow site II in subdomain IIIA) [20, 34] display their characteristic spectral features between 350 and 250 nm. Therefore, competition studies by CD spectroscopy were performed using BV, an ICD marker for the proposed binding site III in subdomain IB of HSA [35].

Upon binding to HSA, the bound conformation of BV displays (*M*)-axial chirality with the onset of a negative ICD band centered around 670 nm and a positive ICD band at 385 nm, both outside the spectral range of Cuc absorption. BV also binds to RSA in (*M*)-conformation: the resulting positive

ICD band for the 1:1 RSA–BV complex (Fig. S4–S5 in the Supplementary Material) lies at the same wavelength as for the 1:1 HSA–BV complex and is relatively more intense (~ +50%).

When CucE and CucI are added to the 1:1 HSA–BV complex, the magnitude of the ICD band for BV at 385 nm slightly increases (Fig. 5): interestingly, the enhancement of the ICD band is more pronounced when CucI is used in the competition study, while the effect of CucE is more limited.

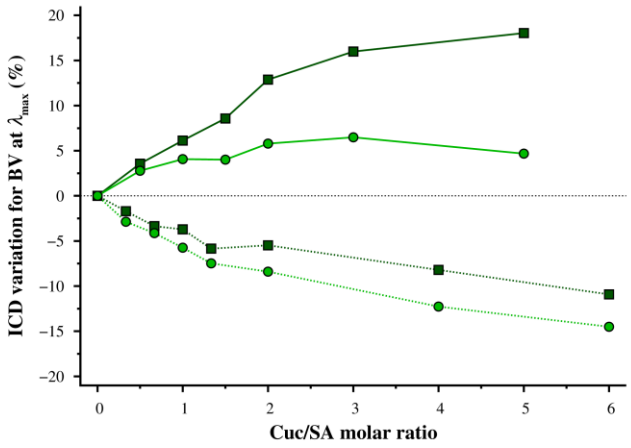

Figure 5. Effect of increasing concentrations of CucE (*circles*) and CucI (*squares*) on the magnitude of the positive ICD band of HSA–BV (*solid lines*) and RSA–BV (*dotted lines*) complexes. Experimental details are reported in the Materials and Methods section and in Tables S3–S4 in the Supplementary Material.

An increase in ICD intensity for a marker is usually indicative of positive allosteric modulation toward the binding site of the marker and an indirect proof of binding for the analyte. Previous investigations on Cuc binding to HSA by fluorescence spectroscopy revealed that CucE enhanced the affinity of bilirubin (BR) toward HSA, while CucI was found to have no effect on HSA–BR binding [36]. BR, the reduced form of BV, binds to the same subdomain IB of HSA and is also, incidentally, one of the most studied ICD markers for high-affinity HSA binding [20, 34].The different effect of CucI on the binding of BR and BV to HSA may seem contrasting. It must be noted, however, that the additional flexibility of the reduced methylene bridge allows for a different binding mode of BR when compared to BV, even though both molecules bind to the same site of HSA; actually, the different signs of the corresponding ICD bands indicate that the stereoselectivity of binding for BR and BV is opposite, with BR binding to HSA with a (*P*)-axial chirality. In some cases, the axial chirality of bound BR can even be inverted through allosteric modulation [37]. The

behavior of CucI confirms the high flexibility of the binding site in subdomain IB and the complex allosteric network regulating the binding of drugs to HSA.

Interestingly, the positive ICD band for BV at 385 nm decreased in intensity when CucE and CucI were added to the 1:1 RSA–BV complex (Fig. 5), suggesting either a competition for the same binding site or a negative allosteric modulation. The available data are not sufficient to discriminate between these two different mechanisms, although the limited extent to which the ICD band for BV is decreased supports the hypothesis of negative allosteric modulation. It is worth noting that the binding of CucE and CucI to serum albumins of different species led to different effects on BV binding, confirming the need for careful investigations on the translation of pharmacokinetic profiles from animal models to humans.

4. Conclusions

The present article reported the investigation on the binding of cucurbitacins E and I to human and rat serum albumins by means of a combination of SPR-based optical biosensing and CD spectroscopic analysis. The steady-state and kinetic analysis of SPR sensorgrams for Cuc–SA complexes unveiled a previously unreported binding event between CucI and HSA, with CucI showing a 3-fold decrease in affinity with respect to CucE. Moreover, the K_d values of CucE and CucI toward RSA resulted to be slightly higher than those observed for HSA, with both compounds binding to RSA with comparable affinity. The calculated percentages of binding allow to rank cucurbitacins E and I as high-affinity binders for both serum albumins. CD spectroscopic analysis showed that cucurbitacins E and I are able to modulate the binding of biliverdin to serum albumins, as observed by the concentration-dependent change in intensity of the positive ICD band of biliverdin upon titration with cucurbitacins. Interestingly, the opposite behaviors observed with HSA and RSA suggest a different type of allosteric modulation by cucurbitacins, positive for HSA and negative for RSA. These observations allow to confirm the usefulness of SPR and CD analysis for the characterization of the pharmacokinetic profiles of drugs and the need for caution in the translation of pharmacokinetic data across species for new drug candidates.

Acknowledgements

The authors thank. FAPESP for the grant 2014/18095-0, São Paulo Research Foundation (G.M.L.F. and L.N.P.), and the University of Bologna (E.F., D.T. and C.B.) for financial support.

References

[1] B. Jayaprakasam, N.P. Seeram, M.G. Nair, Anticancer and antiinflammatory activities of cucurbitacins from *Cucurbita andreana*, Cancer Lett. 189 (2003) 11-16.

[2] J.C. Chen, M.H. Chiu, R.L. Nie, G.A. Cordell, S.X. Qiu, Cucurbitacins and cucurbitane glycosides: structures and biological activities, Nat. Prod. Rep. 22 (2005) 386-399.

[3] G.F. Yuan, M.L. Wahlqvist, G.Q. He, M. Yang, D. Li, Natural products and anti-inflammatory activity, Asia Pac. J. Clin. Nutr. 15 (2006) 143-152.

[4] D.H. Lee, G.B. Iwanski, N.H. Thoennissen, Cucurbitacin: ancient compound shedding new light on cancer treatment, ScientificWorldJOURNAL 10 (2010) 413-418.

[5] K.L.K. Duncan, M.D. Duncan, M.C. Alley, E.A. Sausville, Cucurbitacin E-induced disruption of the actin and vimentin cytoskeleton in prostate carcinoma cells, Biochem. Pharmacol. 52 (1996) 1553-1560.

[6] Y.M. Dong, B.B. Lu, X.L. Zhang, J. Zhang, L. Lai, D.L. Li, Y.Y. Wu, Y.J. Song, J.A. Luo, X.F. Pang, Z.F. Yi, M.Y. Liu, Cucurbitacin E, a tetracyclic triterpenes compound from Chinese medicine, inhibits tumor angiogenesis through VEGFR2-mediated Jak2-STAT3 signaling pathway, Carcinogenesis 31 (2010) 2097-2104.

[7] M.S. van Kester, J.J. Out-Luiting, P.A. von dem Borne, R. Willemze, C.P. Tensen, M.H. Vermeer, Cucurbitacin I inhibits Stat3 and induces apoptosis in Sézary cells, J. Invest. Dermatol. 128 (2008) 1691-1695.

[8] M.H. Jeong, S.-J. Kim, H. Kang, K.W. Park, W.J. Park, S.Y. Yang, D.K. Yang, Cucurbitacin I attenuates cardiomyocyte hypertrophy via inhibition of connective tissue growth factor (CCN2) and TGF-β/Smads signalings, PLoS ONE 10 (2015) e0136236.

[9] T. Peters, Jr., All About Albumin, Academic Press, San Diego, CA, 1996.

[10] G. Sudlow, D.J. Birkett, D.N. Wade, The characterization of two specific drug binding sites on human serum albumin, Mol. Pharmacol. 11 (1975) 824-832.

[11] G. Sudlow, D.J. Birkett, D.N. Wade, Further characterization of specific drug binding sites on human serum albumin, Mol. Pharmacol. 12 (1976) 1052-1061.

[12] T.A.G. Noctor, M.J. Diaz-Perez, I.W. Wainer, Use of a human serum albumin-based stationary phase for high-performance liquid chromatography as a tool for the rapid determination of drug-plasma protein binding, J. Pharm. Sci. 82 (1993) 675-676.

[13] M.J. Banker, T.H. Clark, J.A. Williams, Development and validation of a 96-well equilibrium dialysis apparatus for measuring plasma protein binding, J. Pharm. Sci. 92 (2003) 967-974.

[14] K. Vuignier, J. Schappler, J.-L. Veuthey, P.-A. Carrupt, S. Martel, Drug–protein binding: a critical review of analytical tools, Anal. Bioanal. Chem. 398 (2010) 53-66.

[15] D.S. Hage, J. Anguizola, O. Barnaby, A. Jackson, M.J. Yoo, E. Papastavros, E. Pfaunmiller, M. Sobansky, Z. Tong, Characterization of drug interactions with serum proteins by using high-performance affinity chromatography, Curr. Drug Metab. 12 (2011) 313-328.

[16] G.A. Ascoli, E. Domenici, C. Bertucci, Drug binding to human serum albumin: abridged review of results obtained with high-performance liquid chromatography and circular dichroism, Chirality 18 (2006) 667-679.

[17] C. Bertucci, M. Pistolozzi, A. De Simone, Circular dichroism in drug discovery and development: an abridged review, Anal. Bioanal. Chem. 398 (2010) 155-166.

[18] S. Allenmark, Induced circular dichroism by chiral molecular interaction, Chirality 15 (2003) 409-422.

[19] F. Zsila, Z. Bikadi, I. Fitos, M. Simonyi, Probing protein binding sites by circular dichroism spectroscopy, Curr. Drug Discov. Technol. 1 (2004) 133-153.

[20] D. Tedesco, C. Bertucci, Induced circular dichroism as a tool to investigate the binding of drugs to carrier proteins: classic approaches and new trends, J. Pharm. Biomed. Anal. 113 (2015) 34-42.

[21] Å. Frostell-Karlsson, A. Remaeus, H. Roos, K. Andersson, P. Borg, M. Hämäläinen, R. Karlsson, Biosensor analysis of the interaction between immobilized human serum albumin and drug compounds for prediction of human serum albumin binding levels, J. Med. Chem. 43 (2000) 1986-1992.

[22] C. Bertucci, A. Piccoli, M. Pistolozzi, Optical biosensors as a tool for early determination of absorption and distribution parameters of lead candidates and drugs, Comb. Chem. High Throughput Screen. 10 (2007) 433-440.

[23] A. De Simone, F. Mancini, F. Real Fernàndez, P. Rovero, C. Bertucci, V. Andrisano, Surface plasmon resonance, fluorescence, and circular dichroism studies for the characterization of the binding of BACE-1 inhibitors, Anal. Bioanal. Chem. 405 (2013) 827-835.

[24] C. Fortugno, T. van der Gronde, G. Varchi, A. Guerrini, C. Bertucci, Species-dependent binding of new synthesized bicalutamide analogues to albumin by optical biosensor analysis, J. Pharm. Biomed. Anal. 111 (2015) 324-332.

[25] R.L. Rich, D.G. Myszka, Advances in surface plasmon resonance biosensor analysis, Curr. Opin. Biotechnol. 11 (2000) 54-61.

[26] M.A. Cooper, Optical biosensors in drug discovery, Nat. Rev. Drug Discov. 1 (2002) 515-528.

[27] D.G. Myszka, R.L. Rich, Implementing surface plasmon resonance biosensors in drug discovery, Pharm. Sci. Technol. Today 3 (2000) 310-317.

[28] R.L. Rich, Y.S.N. Day, T.A. Morton, D.G. Myszka, High-resolution and high-throughput protocols for measuring drug/human serum albumin interactions using BIACORE, Anal. Biochem. 296 (2001) 197-207.

[29] D. Zhang, G. Luo, X. Ding, C. Lu, Preclinical experimental models of drug metabolism and disposition in drug discovery and development, Acta Pharm. Sin. B 2 (2012) 549-561.

[30] E.A. Lien, E. Solheim, P.M. Ueland, Distribution of tamoxifen and its metabolites in rat and human tissues during steady-state treatment, Cancer Res. 51 (1991) 4837-4844.

[31] D.G. Myszka, Improving biosensor analysis, J. Mol. Recognit. 12 (1999) 279-284.

[32] F. Hervé, K. Rajkowski, M.T. Martin, P. Dessen, N. Cittanova, Drug-binding properties of rat α_1-foetoprotein. Binding of warfarin, phenylbutazone, azapropazone, diazepam, digitoxin and cholic acid, Biochem. J. 221 (1984) 401-406.

[33] R. Abou-Khalil, A. Jraij, J. Magdalou, N. Ouaini, D. Tome, H. Greige-Gerges, Interaction of cucurbitacins with human serum albumin: thermodynamic characteristics and influence on the binding of site specific ligands, J. Photochem. Photobiol. B 95 (2009) 189-195.

[34] M. Simonyi, Probing HSA and AGP drug-binding sites by electronic circular dichroism, in: N. Berova, P.L. Polavarapu, K. Nakanishi, R.W. Woody (Eds.) Comprehensive Chiroptical Spectroscopy, vol. 2, Wiley & Sons, Hoboken, NJ, 2012, pp. 665-705.

[35] F. Zsila, Subdomain IB is the third major drug binding region of human serum albumin: toward the three-sites model, Mol. Pharm. 10 (2013) 1668-1682.

[36] H. Greige-Gerges, R. Abou Khalil, R. Chahine, C. Haddad, W. Harb, N. Ouaini, Effect of cucurbitacins on bilirubin–albumin binding in human plasma, Life Sci. 80 (2007) 579-585.

[37] C. Bertucci, Enantioselective inhibition of the binding of rac-profens to human serum albumin induced by lithocholate, Chirality 13 (2001) 372-378.